
Article:
Frydrych, M., Roman, S., MacNeil, S. et al. (1 more author) (2015) Biomimetic poly(glycerol sebacate)/poly(L-lactic acid) blend scaffolds for adipose tissue engineering. Acta Biomaterialia, 18. 40 -49. ISSN 1742-7061

https://doi.org/10.1016/j.actbio.2015.03.004

Thermoresponsive, stretchable, biodegradable and biocompatible poly(glycerol sebacate)-based polyurethane hydrogels

*Martin Frydrych[1], Sabiniano Román[2], Nicola H. Green[2], Sheila MacNeil[2] and Biqiong Chen[1]**

[1]Department of Materials Science and Engineering, University of Sheffield, Mappin Street, Sheffield, S1 3JD, United Kingdom.

[2]Kroto Research Institute, Department of Materials Science and Engineering, University of Sheffield, Broad Lane, Sheffield, S3 7HQ, United Kingdom.

ABSTRACT

Thermoresponsive, stretchable, biodegradable and biocompatible polyester-based polyurethane (PEU) hydrogels, based on poly(glycerol sebacate) pre-polymer and poly(ethylene glycol)s of different molecular masses were synthesized by a facile solvent-based two-step method. The chemical and physical characteristics of the PEU hydrogels are tunable, enabling the design of various negatively thermosensitive, mechanically stable and biodegradable systems. The PEU hydrogels demonstrate reversible responses to a change in medium temperature from 5 ^{o}C to 37 ^{o}C, with the swelling ratio at equilibrium varying from 499% to 12%. The hydrogels have a tensile Young's modulus, ultimate tensile strength and elongation at break in the range of 0.02-0.20 MPa, 0.05-0.47 MPa and 426-623%, respectively, and show high stretchability and full shape recovery after compression. These are similar to the mechanical properties of adipose tissues. *In vitro* degradation tests show mass losses of 8.7-16.3% and 10.7-20.7% without and with the presence of lipase enzyme for 31 days, respectively. *In vitro* cell tests show clear evidence that some of the PEU hydrogels are suitable for culturing adipose-derived stem cells and dermal fibroblasts and hence for future soft tissue regeneration. The functionalities of the PEU hydrogels were also evaluated for potential applications in drug delivery, thermal actuation and ultralow power generation. The results demonstrate the versatility of these PEU hydrogels for a variety of biomedical and engineering applications.

KEYWORDS

Thermoresponsive hydrogel; biodegradation; biocompatibility; tissue engineering; drug delivery; actuation.

1. INTRODUCTION

Stimuli-responsive hydrogels are of considerable interest for a range of applications, such as tissue engineering, drug delivery, actuation and sensing, due to their ability to respond to external chemical or physical stimuli.[1] Hydrogels have attractive characteristics, owing to their high water content and three-dimensional (3D) network structure, which closely mimic the natural extracellular matrices of soft tissues.[2] With respect to stimuli-responsive hydrogels, thermoresponsive hydrogels form the most common class, characterized with a temperature-dependent deformation of their polymeric 3D network.[3] Among these hydrogels, thermoresponsive poly(*N*-isopropylacrylamide) (PNIPAm) hydrogels have been extensively investigated, because of their well-defined stimulus sensitivity and transition temperature near the body temperature.[1,3-5] However, the biomedical applications of PNIPAm and its copolymers are restricted due to their non-biodegradability, slow stimuli responsiveness and mechanical weakness.[4,5]

Biodegradable and biocompatible polyurethane (PU)-based thermoresponsive hydrogels have recently received increasing attention.[6,7] PUs offer attractive mechanical properties and have been studied in regenerative medicine applications.[8] They are synthesized from a variety of polyols, diisocyanates, and chain extenders or crosslinkers, offering the flexibility of tailoring their properties to match specific requirements. The thermoresponsive properties of PU-based hydrogels are dependent on the balance of hydrophilic/hydrophobic groups and their interactions with water molecules via hydrogen bonding, in which the polymer chain network collapses or swells in response to the change in temperature of the aqueous medium.[1,9] Poly(ethylene glycol) (PEG) is one of the most used polyols for designing PU-based hydrogels and it has been approved for use in medical applications by the U.S. Food and Drug Administration (FDA).[10,11]

PEG presents attractive physicochemical and biological properties, including hydrophilicity, solubility in water and polar organic solvents, non-toxicity and non-immunogenicity.[2,12] Hence, the modulation of PU-based hydrogels with PEG improves the biocompatibility, and enables the adjustment of degradability and mechanical properties by varying the molecular mass or concentration of the PEG.[7,13]

The ability to design PU-based hydrogels using a biodegradable and biocompatible polymer building block, either natural[2,12,14] or synthetic,[2,12,15,16] is an essential feature in tailoring their biodegradability and biocompatibility. Natural polymers are generally biocompatible, however their poor mechanical properties, fast degradation rates, poor reproducibility and potential immunogenicity restrict their use.[2] In contrast, synthetic polymers have more predictable and reproducible physical and biological properties.[2] Poly(glycerol sebacate) (PGS) is a synthetic biodegradable and biocompatible elastomer, specifically designed for soft tissue applications.[17,18] It is synthesized via a polycondensation reaction of glycerol and sebacic acid, forming a meltable and soluble pre-polymer (pre-PGS) which subsequently cures to create a covalently crosslinked PGS network.[17,18] PGS can sustain and recover from deformations in mechanically dynamic environments, which is attributed to its 3D molecular structure and elastomeric nature.[19] PGS is bioresorbable and both of its monomers haven been approved by the FDA for the utilization in medical applications.[17] Previous *in vitro* and *in vivo* studies have demonstrated good cell compatibility with minimal inflammatory response to PGS implants,[17,20-22] as well as relatively linear degradation kinetics and good retention of mechanical strength during degradation due to its surface erosion patterns.[17,20-22] While PGS itself exhibits tunable properties,[18] the functional hydroxyl groups of PGS also allow one to incorporate different functionalities by reacting with the hydroxyls and hence tailoring its physiochemical properties, as shown by recently developed PGS-based copolymers, blends and composites.[18,23-26] For instance, hydrophilic segments such as

citric acid or PEG were successfully incorporated into the PGS backbone, resulting in PGS-based copolymers with improved and tunable hydrophilic properties,[24,26,27] and the use of isocyanate-based crosslinkers allowed researchers to design mechanically highly tunable PU-based elastomers under mild reaction conditions.[23] However, most of these studies aimed to either improve the processability of PGS, or modify the mechanical properties, degradation behaviour or hydration properties of PGS.[18] While pristine PGS has been recently investigated for basic one-way shape-memory effects,[28] the development of reversibly stimuli-responsive PGS-related hydrogels has not been reported.

In this work, we report novel thermoresponsive, stretchable and biodegradable polyester-based polyurethane (PEU) hydrogels, synthesized from pre-PGS and PEGs of different molecular masses (MWts), both containing hydroxyl groups, with aliphatic hexamethylene diisocyanate (HDI). HDI was selected due to its extensive use in synthesizing biocompatible polyurethanes.[23,29] We hypothesized that the synthesis of the PEU using (I) biodegradable pre-PGS as the main macromolecular crosslinker, (II) hydrophilic PEG as the main polyol component, and (III) hydrophobic HDI as the diisocyanate component, could create a chemically crosslinked thermoresponsive hydrogel with the combined advantages of PGS, PEG and PU. By varying the MWt of PEG, the chemical and physical characteristics of the PEU hydrogels could be tailored. The structure and properties of these thermoresponsive materials were investigated, and their potential applications for tissue engineering, drug delivery and thermal actuation were evaluated. The structure of the PEUs was characterized by spectroscopic and calorimetric measurements, the mechanical properties were analyzed via quasi-static and cyclic tensile and compression tests, and the hydration kinetics and swelling behavior were studied under various medium temperatures. *In vitro* degradation tests were carried out in media with and without lipase, and cell proliferation response was examined *in vitro* with human adipose-derived stem

cells (ADSCs) and dermal fibroblasts (FIBs). Drug encapsulation and release as well as temperature-induced actuation behaviour were studied. The potential of fabricating the PEU material into different forms such as microspheres and large 3D porous scaffolds was also demonstrated.

2. MATERIALS AND METHODS

2.1 Materials

Sebacic acid, glycerol, HDI, Tin (II) 2-ethylhexanoate (Tin (II)), PEG (with the number average molar mass ($\bar{M}_n$) of 400 g mol^{-1} (PEG-400), 950-1050 g mol^{-1} (PEG-1000) and 1305-1595 g mol^{-1} (PEG-1450)), dimethylformamide, 1,4-dioxane, acetone, diemethyl carbonate, toluene, tetrahydrofuran (THF), chloroform, ethanol, hexane, mineral oil, Span 80, n-heptane, lidocaine, phosphate buffered saline (PBS) tablets (for preparing a PBS-water solution of pH 7.4), lipase from porcine pancreas (54 U mg^{-1}), Dulbecco's modified Eagle's medium (DMEM), trypsin-ethylenediaminetetraacetic acid (Trypsin/EDTA), formaldehyde, phalloidin-fluorescein isothiocyanate (phalloidin-FITC) and resazurin were purchased from Sigma-Aldrich. Fetal calf serum (FCS), penicillin-streptomycin, glutamine and amphotericin B were purchased from Gibco. Collagenase type A was acquired from Roche Diagnostics GmbH. Difco-trypsin plus was obtained from Difco Laboratories.

2.2 Synthesis and Characterization of PGS Pre-polymer

Pre-PGS was synthesized according to published methods,[17,30] by reacting a 1:1 molar mixture of sebacic acid and glycerol at 120 °C for 72 h under a low flow of nitrogen gas and at constant stirring. The $\bar{M}_n$, the mass average molar mass ($\bar{M}_w$) and the polydispersity index (*PDI*) of pre-

PGS were measured by gel permeation chromatography (GPC) using an Erma ERC-7512 Refractive Index detector and calibrated with polystyrene standard samples.

2.3 Solvent-based Synthesis of PEUs

PEUs were synthesized by using a solvent-based two-step approach with a fixed molar ratio (glycerol : isocyanate (NCO)-terminated PEG = 1 : 0.30). Briefly, the first step involved the reaction of PEG (1 mmol; PEG-400, PEG-1000 or PEG-1450) and HDI (2 mmol) in 1,4-dioxane (20 mL) with Tin (II) (0.05% w/v) as the catalyst for 1 h at 85 °C. In the second step the NCO-terminated PEG/1,4-dioxane solution was cooled down to 55 °C, to which a pre-PGS solution (3.4 mmol pre-PGS in 20 mL 1,4-dioxane with 0.05% w/v Tin (II)) was added and reacted for 5 h. At each step the reaction flasks were purged with nitrogen and sealed. The reacted solution was poured onto a non-sticky mould and the solvent was allowed to evaporate for 2 days at room temperature and another 2 days in a vacuum oven at 40 °C, which also allowed for further crosslinking. All the specimens were subjected to a cleaning procedure (24 h ethanol saturation and drying in a vacuum oven at 37 °C) prior to tests to remove unreacted pre-polymer and monomers. The nomenclature of the synthesized hydrogels is presented as PEU-X, where "X" represents $\bar{M}_n$ of the utilized PEG: PEU-400, PEU-1000 and PEU-1450.

2.4 Characterization of PEUs

Proton nuclear magnetic resonance spectroscopy (^{1}H NMR) was performed on a Bruker Avance III HD 500, and samples were recorded at 25 °C at 500 MHz, using deuterated chloroform ($CDCl_3$) as the solvent. PEUs were soaked overnight in $CDCl_3$ and the acquired ^{1}H NMR data were analyzed using ACDLABS/1D NMR software. Attenuated total reflectance Fourier Transform Infrared Spectroscopy (ATR-FTIR) was performed on a Perkin Elmer Spectrum One

NTS analyzer, operated in the mid-infrared region of 4000-450 cm^{-1} and recorded with a resolution of 1 cm^{-1}. Raman spectroscopy was executed on a Renishaw inVia Raman spectroscope using a 514.5 nm wavelength laser. Spectra were recorded between 500-3500 cm^{-1} with a laser power of 2 mW and a spectral resolution of 0.5 cm^{-1}. Differential Scanning Calorimetry (DSC) was carried out on a Perkin Elmer Diamond DSC, and temperature scans from -60 °C to 120 °C at 10 °C min^{-1} under a nitrogen flow rate of 20 ml min^{-1} were performed during two consecutive heating cycles. The heat capacity change in the second heating cycle was used for analysis.

The solubility of PEU film specimens was evaluated by immersing the specimens in a solvent, 1.4-dioxane, dimethylformamide, diemethyl carbonate, toluene, chloroform, acetone or ethanol, for 24 h at 21 °C. The sol contents of non-cleaned PEU film specimens (n = 5) were calculated by determining the mass difference after 24 h ethanol saturation at 21 °C.

Quasi-static tensile and compression tests were performed on dry and hydrated PEU film specimens (hydrated PEU specimens (donated as hydrogels herein) had been immersed in PBS solution for 24 h at 37 °C and were immediately removed from the solution for the tests), while cyclic tensile and compression tests were conducted on PEU hydrogels. Briefly, quasi-static uniaxial tensile tests were carried-out with a 10 N load cell on a Hounsfield H100KS mechanical testing machine (Tinius Olsen, USA), at a tensile strain rate of 50 mm min^{-1} till fracture (ASTM D412) with “dog bone” shaped specimens (n = 8; width: 2.6 mm, gauge length: 20 mm, thickness: 0.42-1.29 mm). Cyclic tensile tests (n = 3; width: 2.6 mm, gauge length: 20 mm, thickness: 0.82-1.65 mm) were performed under the same testing set-up at a tensile strain rate of 50 mm min^{-1} and stretched to 50% strain during 20 cycles. Quasi-static uniaxial compression tests were executed on cylindrical specimens (n = 7; diameter: 6 mm; thickness: 1.10-3.72 mm) with a 1 kN load cell up to a strain of 75% and a strain rate of 1 mm min^{-1}. Cyclic compression

tests (n = 3; diameter: 6 mm; thickness: 1.09-3.57 mm) were performed under the same testing set-up at a strain rate of 1 mm min^{-1} and compressed to 50% strain during 20 cycles. All the tests were performed at ambient conditions (21 °C).

Hydration kinetics and swelling behaviour of dried PEU film specimens (n = 5) were analyzed at various medium temperatures for up to 48 h. Dry specimens of initial known mass were immersed in PBS solution at constant 5 °C, 21 °C or 37 °C, which represent three important temperature conditions of possible storage or application environments (e.g. fridge (5 °C), room temperature (21 °C) and human body temperature (37 °C)). At specific time intervals, swollen specimens were taken out of the medium, with excessive surface water removed and their swollen mass determined, and the tests was continued until the specimens reached the stage of equilibrium. The mass swelling ratio was determined by the difference between the masses of the swollen sample and the initial dry sample divided by the mass of the initial sample. The reversible swelling/deswelling behavior of dried PEU film specimens (n = 5) was analyzed in PBS solution at alternating temperatures of 5 °C and 50 °C, at an interval of 40 min for up to 4 h.

In vitro degradation studies were performed on PEU film specimens (n = 3; thickness: 0.57 ± 0.10 mm; width: 2.5 ± 0.03 mm; length: 4.8 ± 0.02 mm), based on our previous work.[31,32] Briefly, tests were performed in a shaker incubator (Stuart SI500; 100 rpm) at 37 °C in two separate degradation media: a lipase-containing PBS solution (110 U L^{-1}; serum lipase in healthy adults is in the range of 30-190 U L^{-1})[33] and an enzyme-free PBS solution as control. Both degradation media were changed every day to maintain enzymatic activity. The specimens were removed from the degradation medium after 1, 3, 7, 11, 15, 19, 23, 27 and 31 days of incubation, washed with distilled water, dried in a vacuum oven at 37 °C, and weighed. Scanning electron microscopy (Camscan S2; SEM) was performed on the specimens after 31 days' *in vitro*

degradation, as well as on untreated samples, at 5 kV. The specimens were gold coated for 3 min at 15 mA by using a sputter coater (Emscope SC500).

2.5 Drug Encapsulation and Release Tests of PEUs

For the drug encapsulation, dry punched-out PEU film specimens (n = 5; diameter: 6 mm; thickness: 0.74 ± 0.18 mm) were soaked in a lidocaine solution (0.01 g mL^{-1} PBS, 10 mL) for 48 h at 5 °C. The swollen specimens were removed and dried in a vacuum oven for 24 h at 37 °C. The lidocaine-loaded samples were then immersed in PBS (10 mL) in a shaker incubator (100 rpm) at 37 °C. At several time intervals, 1 mL was removed and replaced by the same volume of fresh PBS. The cumulative drug release rate was calculated by evaluating the characteristic absorbance peak of lidocaine at 263 nm against a calibration curve of lidocaine-containing PBS solutions at known concentrations.

2.7 *In Vitro* Cell Culture Experiments

Skin and associated fat were obtained with informed consent from patients undergoing elective surgery for breast reductions or abdominoplasties, from tissue not required for their treatment donated for research. All donated tissues were handled on an anonymous basis, under a Human Tissue Authority research tissue bank license (number 08/H1308/39). Human subcutaneous fat from discarded skin was selected as the ADSC source. Mechanical and enzymatic (collagenase type A) digestion was followed by several washes, and the stromal vascular fraction was cultured in DMEM (supplemented with 10% FCS, 100 IU ml^{-1} penicillin-streptomycin, 100 µg ml^{-1} glutamine and 0.625 µg ml^{-1} amphotericin B). The human ADSCs were subcultured to passage 4 for use in the experiments. Human skin biopsies were treated enzymatically (Difco-trypsin plus) to separate the dermis. FIBs were obtained after collagenase treatment (collagenase type A) from

finely minced dermis and cultured in supplemented DMEM. The human skin FIBs were subcultured to passage 9, as described previously.[34]

Experiments were performed in triplicate. Briefly, PEU specimens (diameter: 15 mm) were placed in a 12-well plate and sterilized with 0.1% peracetic acid in PBS overnight. Then, specimens were washed 3 times with PBS (1 h each) and dried overnight in a sterile laminar flow culture hood under UV light. The sterilized and dried specimens were soaked in DMEM overnight in an incubator (37 ºC, 5% CO_2), and fixed with a metal ring (internal diameter: 10 mm) for cell seeding. After cell trypsinisation with Trypsin-EDTA, ADSCs (5 x 10^4 cells per sample) and FIBs (5 x 10^4 cells per sample) were seeded onto the PEU specimens with DMEM (cell-free specimens were included as controls in DMEM). After 2 h incubation (37 ºC, 5% CO_2), rings and DMEM were removed and a metabolic activity assay was performed (1 ml of resazurin (5 μg mL^{-1} in PBS) was added to each well and incubated for 60 min). The absorbance at 570 nm was measured in a colorimetric plate reader (Bio-TEK). Resazurin was then removed and samples returned to culture conditions with 2 mL of DMEM. This metabolic assay was repeated on days 3, 6 and 9 and images of the well plates were taken after each incubation. After the final incubation, all samples were washed in PBS and fixed with 3.7% formaldehyde in PBS for 15 min. After 3 PBS washes, the samples were incubated in 2 mL phalloidin-FITC (diluted 1:500 in PBS) for 30 min. After 3 further PBS washes, images (512x512 pixels) were obtained using a Zeiss LSM 510Meta inverted confocal microscope and W N-Achroplan 40x 0.75 NA objective, with a 12.8 μs pixel dwell time. FITC was excited using a 488 nm laser and emission detected between 500 and 550 nm.

2.8 Water Temperature Activated Force Generation Measurements

Water temperature activated force generation was evaluated on PBS saturated (at 21 °C for 48 h) and stretched (constant strain = 40 %) PEU-1450 strip samples (n = 2; thickness: ~1.45 mm; width: 8 mm; gauge length: 20 mm) (See Figure S1A for the test set-up). During the testing period water temperature was alternated between 21 °C and 37 °C, or 5 °C and 37 °C, with an interval of 10 min for up to 70 min. This was accomplished by exchanging the same volume of water (of the desired temperature) rapidly. The force was measured with a 10 N load cell on a Hounsfield H100KS mechanical testing machine.

2.9 Water Temperature Responsive Cantilever Tests

A two-layer cantilever was constructed from a pre-hydrated PEU-1450 (24 h PBS saturation at 21 °C; thickness: ~2.1 mm; width: 5 mm; gauge length: 50 mm) and a flexible poly(tetrafluoroethylene) (PTFE) film strip (Figure S1B). The two strips were connected to each other at both ends only using an adhesive. The PTFE side was further fixed with adhesive to the centre of a screw tip, allowing both strip ends to move freely. The test was performed according to the following steps. The cantilever was first placed in cold PBS (5 °C) for 15 min (low medium temperature = PEU hydrogel swelling). The test started by adding hot PBS (95 °C), until the medium exchange resulted in a stable high temperature of ~90 °C (high medium temperature = PEU hydrogel deswelling). After 3 min cold PBS (5 °C) was added until a low temperature of ~5 °C was reached. The test was completed within 6 min.

2.10 Statistics

All measurements were reported as mean ± standard deviation (SD) with a confidence level of 95%. Differences were statistically tested against a null hypothesis of no difference between samples using a two-sample *t*-test (two-tailed) with equal variance not assumed. Two-way

analysis of variance (ANOVA) was used to determine the differences in metabolic activity of the *in vitro* cultured ADSCs and FIBs in respect to test time and material. A p value < 0.05 was considered to be statically significant.

3. RESULTS AND DISCUSSION

3.1 Synthesis and Characterization of PEUs

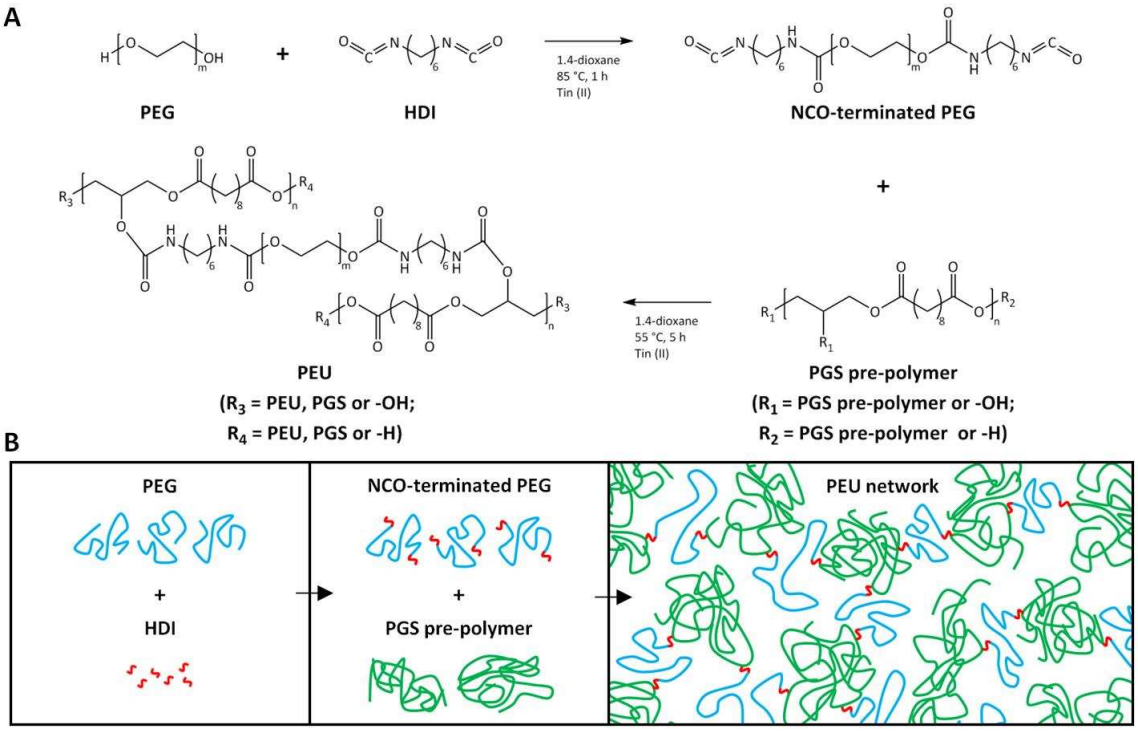

Figure 1. (A) Synthesis scheme of PEUs. (B) Sketch showing the formation of the PEU network.

Chemically crosslinked PEU hydrogels were synthesized using a solvent-based two-step approach with a fixed molar ratio (glycerol : NCO-terminated PEG = 1 : 0.30) (Figure 1A-B). The first step involved the synthesis of NCO-terminated PEGs, by reacting PEG ($\bar{M}_n$ = 400, 1000 or 1450) with HDI in 1.4-dioxane. In the second step, pre-synthesized pre-PGS was dissolved in 1.4-dioxane and added to the NCO-terminated PEG solution to produce PEU

through the crosslinking reaction between the hydroxyl groups of the pre-PGS units and the –NCO groups from the functionalized PEG. The pre-PGS in use had a $\overline{M}_n$, $\overline{M}_w$ and *PDI* of 1549 g mol^{-1}, 10522 g mol^{-1} and 6.8 respectively, as determined by GPC.

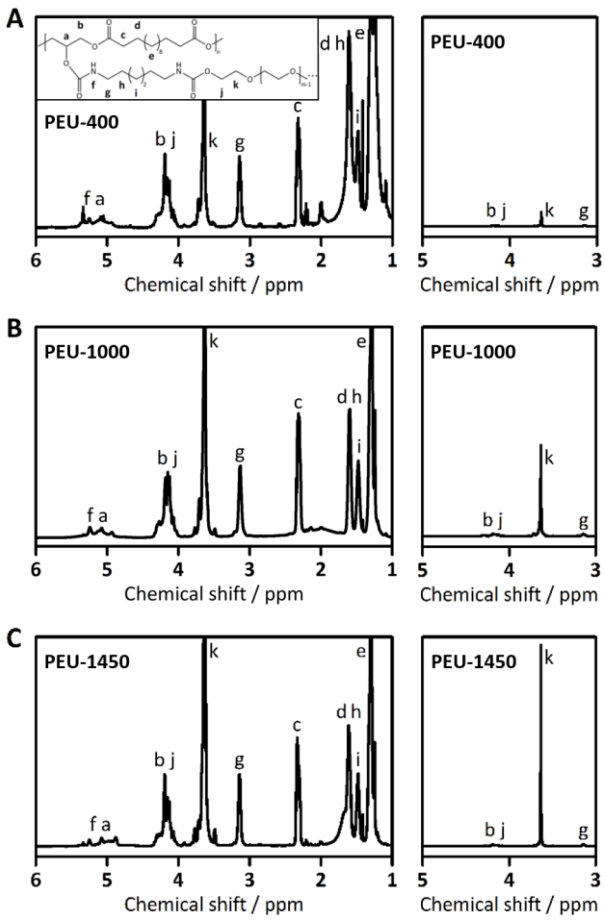

Figure 2. Normalized ^{1}H NMR spectra of (A) PEU-400, (B) PEU-1000 and (B) PEU-1450. The figures on the right show the methylene proton related peak of PEG, "k", increases with its increasing molecular mass.

The molecular structure of the PEUs synthesized using three different molecular masses of PEG was confirmed by ^{1}H NMR spectroscopy (Figure 2), characterized with distinctive peaks of pre-PGS and PEGs (Figure S2), as well as urethane related peaks due to the reaction between pre-PGS and the NCO-terminated PEGs. Characteristic peaks of pre-PGS related methylene

protons were assigned at 1.29, 1.61 and 2.32 ppm (position "e", "d" and "c") for sebacic acid, while peaks from 4.05-4.35 ppm and 4.92-5.24 ppm (position "b" and "a") were linked to the methylene protons of glycerol.[27,35] The methylene proton related peaks of PEG were assigned at 3.63 ppm (position "k") and 4.05-4.35 ppm (position "j", which overlaps position "b").[27] The intensity of peak "k" increased with enhanced MWt of PEG (Figure 2, Right), confirming the presence of a higher mass of PEG segments within the PEU. The peaks at 1.48 ppm, 1.61 ppm, 3.12 ppm and 5.34 ppm (position "i", "h", "g" and "f") were assigned to urethane and HDI related methylene protons, highlighting urethane bonds. Compared to the glycerol related peaks in the ^{1}H NMR spectra of pre-PGS (Figure S2), the ^{1}H NMR data of PEUs presented increased integral signals at 4.92-5.24 ppm (position "a"), indicating that the urethane-bond formation between the NCO-terminated PEGs and the free hydroxyl groups of pre-PGS occurred preferentially with the hydroxyl groups of glycerol.[35]

The analysis of ATR-FTIR spectra of PEUs (Figure 3A), pre-PGS and PEGs (Figure S3) supported the ^{1}H NMR results. The spectra of PEUs showed the stretching vibrations of N-H at 3360 cm^{-1}, C=O at 1723 cm^{-1}, amide III at 1241 cm^{-1}, C-O at 1093 cm^{-1}, C-O-C at 948 cm^{-1}, and amide IV at 842 cm^{-1}, as well as the bending vibrations of amide II at 1532 cm^{-1}, confirming the formation of urethane linkages.[7,17,36] In contrast, ATR-FTIR spectra of NCO-terminated PEGs (Figure S3) were characterized with the stretching vibration of HDI related –NCO end groups at 2270 cm^{-1}, the stretching and bending vibrations of urethane-bond linked C=O and amide II at 1723 cm^{-1} and 1537 cm^{-1}, and the stretching vibration of PEG associated C-O-C at 950 cm^{-1}, showing the unreacted residual –NCO groups at the chain ends and the urethane-bond formation between HDI and PEG.[7,36] The absence of –NCO band at 2270 cm^{-1} in all the three spectra of the PEUs indicates the complete reaction of the –NCO end groups from the PEG with the hydroxyls of pre-PGS.

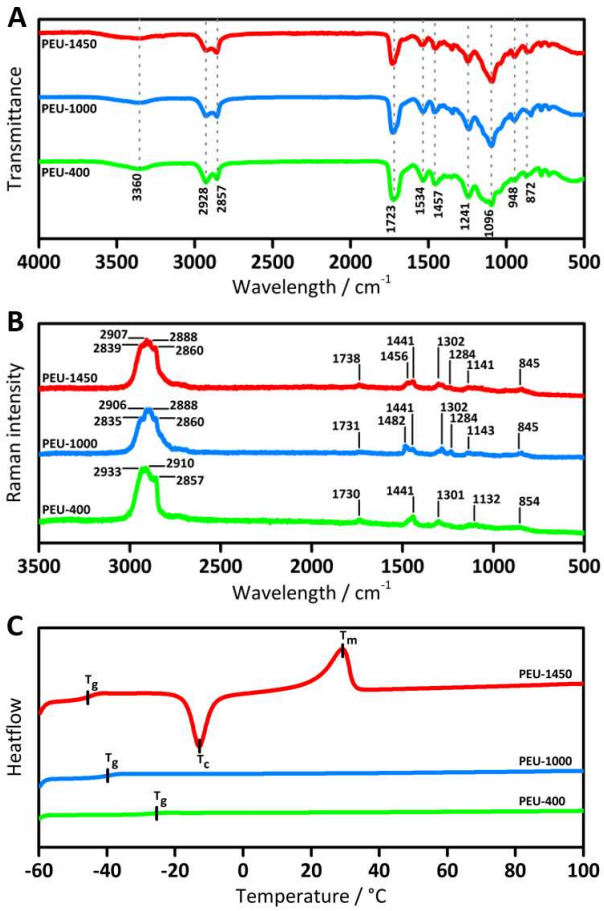

Figure 3. (A) ATR-FTIR spectra, (B) Raman spectra, and (C) DSC curves of PEUs. The spectra/curves were shifted vertically for clarity.

Raman spectra analysis of PEUs (Figure 3B) also affirmed the above ^{1}H NMR and ATR-FTIR results. The spectra of PEUs showed the stretching vibrations of CH_2 in the range of 2700-3000 cm^{-1}, C=O at ~1731 cm^{-1}, the bending vibrations of CH_2 and CH_2-CH_2 in the range of 1200-1500 cm^{-1}, the stretching vibration of C-O at ~1140 cm^{-1} and the rocking vibration of CH_2 at 843 cm^{-1}.[37-39] Comparing the spectra of the PEUs with pre-PGS and PEGs (Figure S4) showed a decrease of the pre-PGS related stretching vibration of C-O at 1102 cm^{-1}, as well as the disappearance of the PEG linked twisting vibration peaks of C-O-H at ~533 cm^{-1} and ~581 cm^{-1}, which are associated to the hydrogen bond reduction due to the formation of urethane bonds.[37-39]

No peaks for unreacted -NCO urethane groups were detected in the spectra of PEUs, confirming the establishment of urethane linkage.

The thermal properties of the PEUs and their main individual components were analyzed by DSC (Figure 3C and S5). PEUs presented glass transition temperature (T_g) values below 0 °C, which decreased with the incorporation of longer PEG chains due to higher chain mobility (PEU-400: T_g = -27.7 °C; PEU-1000: T_g = -40.3 °C; PEU-1450: T_g = -45.2 °C). No crystallization temperature (T_c) or melting temperature (T_m) was detected for PEU-400 and PEU-1000 specimens within the test range, owing to the lower-molecular-mass PEG segments, which yield restricted chain mobility and no crystallization in the PEU network.[40] However, T_c and T_m were observed in PEU-1450 specimens (T_c = -12.9 °C; T_m = 29.1 °C), owing to the presence of the semi-crystalline PEG-1450 in the network.[7] Pre-PGS presented three T_m peaks at -7.6 °C, 14.4 °C and 33.4 °C, which is typical for pre-PGS in its partially crosslinked state and depends on its synthesis procedure.[20,41] PEG-400 exhibits a low T_m of 2.1 °C, while PEG-1000 and PEG-1450 presented higher T_m values of 39.9 °C and 50.8 °C (Figure S5), respectively. The T_m observed for the PEU-1450 specimen was lower than that from neat PEG-1450, indicating that the chemically crosslinked network and the reduced chain mobility affected the crystallization of the PEG-1450 segments.[42] Overall, the results reveal that the MWt of PEG affects the thermal transition of the PEU.

All the PEUs were insoluble in various organic solvents (1,4-dioxane, dimethylformamide, diemethyl carbonate, toluene, chloroform, acetone and ethanol) and only showed strong swelling after immersion for 24 h, confirming the formation of a covalently crosslinked network. Residual analysis of PEU-400, PEU-1000 and PEU-1450 specimens gave mass losses of 23.6 ± 2.4%,

24.7 ± 0.5% and 24.5 ± 7.7% respectively, after 24 h ethanol extraction, indicating the existence of non-crosslinked components.

3.2 Mechanical Properties of PEUs

Table 1. Tensile and compression properties of PEUs.

		Tensile				Compression	
	Sample code	Young's modulus, E_t / MPa	Ultimate tensile strength, σ_{tmax} / MPa	Elongation at break, ε_{tb} / %	Energy at break, T / MJ m^{-3}	Young's modulus, E_c / MPa	Comp. stress at $\varepsilon_{c75\%}$, $\sigma_{c75\%}$ / MPa
Dry	PEU-400	0.72 ± 0.01	0.70 ± 0.02	438 ± 7	1.63 ± 0.07	1.86 ± 0.81	12.68 ± 1.01
	PEU-1000	0.71 ± 0.14	0.49 ± 0.04	400 ± 67	1.03 ± 0.17	0.80 ± 0.07	9.36 ± 2.55
	PEU-1450	13.11 ± 2.22	1.59 ± 0.25	505 ± 77	6.78 ± 0.93	17.91 ± 0.77	16.36 ± 2.86
Hydrated	PEU-400	0.20 ± 0.11	0.47 ± 0.11	426 ± 44	1.09 ± 0.10	1.44 ± 0.22	10.39 ± 1.37
	PEU-1000	0.03 ± 0.01	0.05 ± 0.01	497 ± 153	0.19 ± 0.03	0.44 ± 0.17	4.60 ± 0.86
	PEU-1450	0.02 ± 0.01	0.07 ± 0.01	623 ± 193	0.23 ± 0.04	0.10 ± 0.02	0.67 ± 0.07

The mechanical properties of PEUs were determined under dry and hydrated states by quasi-static tensile and unconfined compression tests, while cyclic tensile and compressive testing were also performed for hydrated PEU hydrogels (Figure 4 and S6, Table 1). The quasi-static mechanical properties of dry PEU-400 and PEU-1000 were similar under tensile load, while dry PEU-1450 shows significantly higher mechanical properties, with the tensile Young's modulus, tensile strength, elongation at break of 13.11 MPa, 1.59 MPa and 505%, respectively (Figure 4A). Correspondingly, dry PEU-400 and PEU-1000 were comparatively flexible, whereas the PEU-1450 specimens were more rigid. Moreover, dry PEUs demonstrated significant differences

in compressive Young's modulus and compressive stress at 75% strain, with the dry PEU-1450 specimens again showing the highest stiffness (Figure 4B). This can be accounted for by the presence of the semi-crystalline PEG-1450 with the highest molecular mass in the PEU network, as previously confirmed by DSC results.

With respect to the mechanical properties of hydrated PEU hydrogels, complex deformations such as knotting and stretching could be performed on all the PEU hydrogels without fracture (Figure 4C), demonstrating excellent flexibility and stretchability. One of the main issues with most hydrogels is their mechanical weakness.[4,5] Ideally, hydrogels for soft tissue engineering should be structurally stable and flexible to withstand mechanical forces and deformations in demanding *in vivo* environments.[4,5] Tensile test results of PEU hydrogels indicated that an increase in PEG MWt from 400 to either 1000 or 1450 led to a decrease with statistical significance ($p < 0.05$) in the tensile Young's modulus and tensile strength as well as a significant increase in the tensile energy at break of the PEU hydrogel. PEU-1450 hydrogels presented the lowest Young's modulus of 0.02 MPa, a tensile strength of 0.07 MPa, and the highest elongation at break of 623% (Figure 4D). Furthermore, all the PEU hydrogels could be compressed to a high strain (75%) without fracture and recover their original shape upon the release of the load (Figure 4E and S6). The PEU hydrogels presented significant differences in compressive Young's modulus and compressive stress at 75% strain. The PEU-1450 hydrogel demonstrated the softest characteristics overall.

The effective crosslink density (n_{eff}) of the PEU hydrogels was calculated from compressive testing results (based on 24 h saturation in PBS at 37 °C) by Equation 1 and S1-3,[43,44]

$$\sigma_c = n_{eff} RT \phi_2^{1/3} \phi_0^{2/3} (\alpha - \alpha^{-2}) \quad (1)$$

where σ_c is the applied force of per unit area of swollen hydrogel during compression, R is the gas constant, T is absolute temperature, ϕ_2 is the polymer volume fraction in the swollen state, ϕ_0 is the polymer volume fraction in the gel in the relaxed state, and α is the deformation ratio ($\alpha = L/L_0 \geq 0.95$) under compression. The values of n_{eff} were calculated as 322, 64 and 11 mol m^{-3} for PEU-400, PEU-1000 and PEU-1450 hydrogels, respectively. The decrease of the tensile strength and Young's modulus, as well as the increase of elongation at break in the PEUs with higher MWts is a consequence of the increase in the chain length between the neighbouring crosslinks, lowering the n_{eff} in the hydrogels and improving their flexibility, which correlates with the swelling properties of the hydrogels[2] discussed in Section 3.3.

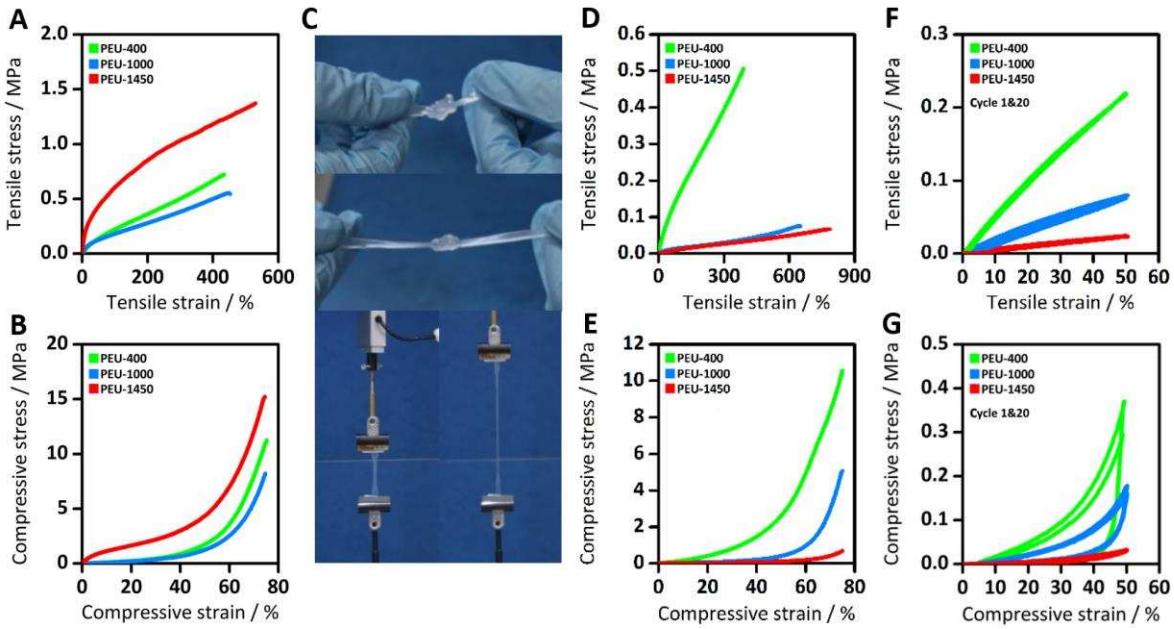

Figure 4. Representative quasi-static (A) tensile and (B) compression stress-strain (test terminated at a compressive strain of 75%) curves of dry PEUs. (C) Mechanical knotting and stretching reliability of PEU-1450 hydrogel specimens. Representative quasi-static (D) tensile and (E) compression stress-strain curve of PEU hydrogels. Representative cyclic (F) tensile and (G) compression stress-strain curves of PEU hydrogels.

Cyclic stress-strain curves of PEUs were characterized with a hysteresis loop during tensile and compression tests (Figure 4F-G). The hysteresis, or dissipated energy (e_d), was determined by evaluating the area between the loading and unloading curves during cyclic tensile or compression tests, and a hysteresis loss ratio (h_r) was defined by Equation 2,[45]

$$h_r = \frac{e_0 - e_r}{e_0} = \frac{e_d}{e_0} \quad (2)$$

where e_0 and e_r are the input and retraction strain-energy densities, respectively. Under cyclic tensile testing, minimal h_r was observed for all the PEU hydrogels. The PEU-400, PEU-1000 and PEU-1450 hydrogels were characterized with h_r values of 0.06, 0.11 and 0.15 after 20 cycles of tensile loading to 50% strain, respectively. In respect to cyclic compression testing, PEU-1450 specimens showed a h_r of 0.31, while the PEU-400 and PEU-1000 specimens presented higher degrees of h_r of 0.74 and 0.55 after 20 cycles of compression loading to 50% strain (Figure 4G), respectively. The expelling of water from the hydrogel observed during the loading cycles presumably contributed to the higher hysteresis loss under compression.

Overall, the PEU hydrogels reported here show excellent performance under quasi-static and cyclic tensile and compressive loads. They are structurally stable, highly stretchable and suitable to engineer scaffolds for a range of soft tissues, such as human cardiac muscles (Young's modulus: 0.01-0.30 MPa)[46] or high stress adapted adipose tissue (Young's modulus: 0.02-0.18 MPa)[47] due to their similar mechanical properties. The incorporation of PEG segments with different MWts into the PEU hydrogel altered mechanical properties. The PEG segment with a higher MWt improved the flexibility and stretchability of the PEU hydrogel, while reducing their strength and modulus, mainly due to its lower crosslink density and higher water uptake (see below).

3.3 Swelling Properties of PEUs

The hydration behaviour of the PEUs was evaluated in PBS at 5, 21 and 37 °C (Figure 5A-E). The mass swelling ratio of the PEUs increased rapidly within the first 12 h, and gradually reached a plateau after 24 h (Figure 5B-D). At 5 °C, PEU-400, PEU-1000 and PEU-1450 presented the highest ratios of swelling at equilibrium of 31%, 207% and 499%, respectively, among the three test temperatures. PEU-400, PEU-1000 and PEU-1450 reached swelling ratios at equilibrium of 20%, 154% and 426% at 21 °C, and of 12%, 113% and 235% at 37 °C, respectively. The difference in the swelling ratio of the PEU hydrogels between low and high test temperatures is statistically significant ($p < 0.05$). The PEUs presented negative thermo-sensitivity, and the equilibrium ratio of swelling depended on the medium temperature as well as the hydrophilic/hydrophobic segment composition of the PEUs. The swelling capacities of the PEUs increased with higher MWt PEGs, due to the increased chain length between the crosslinks as discussed previously and the increased hydrophilicity of the PEGs.[7] Analysis of the dynamic swelling/deswelling behavior of the PEU hydrogels demonstrated repeatable and reversible response to alternating medium temperatures (Figure 5F). At lower medium temperatures the hydrogen bonding between hydrophilic PEU polymer segments and the water molecules are dominating, while at higher medium temperatures the hydrophobic interactions between the PEU polymer segments are enhanced (due to the increased intrinsic affinity of the polymer chains), causing the secretion of hydrated water molecules from the PEU network.[1,9] The PEUs presented relatively high swelling rates, while the deswelling rates were slightly lower, which can be in part associated with the alternation of the matrix permeability during the change of the medium temperature.[48] The swelling/deswelling rates depend on the specific surface area of the specimen, the composition of the hydrogel and the environmental conditions. These results also indicated

that the PEUs with higher MWt PEGs would respond with greater swelling/deswelling rates upon minor changes of temperature, thus making these PEU hydrogels more attractive for potential thermosensitive actuation applications.

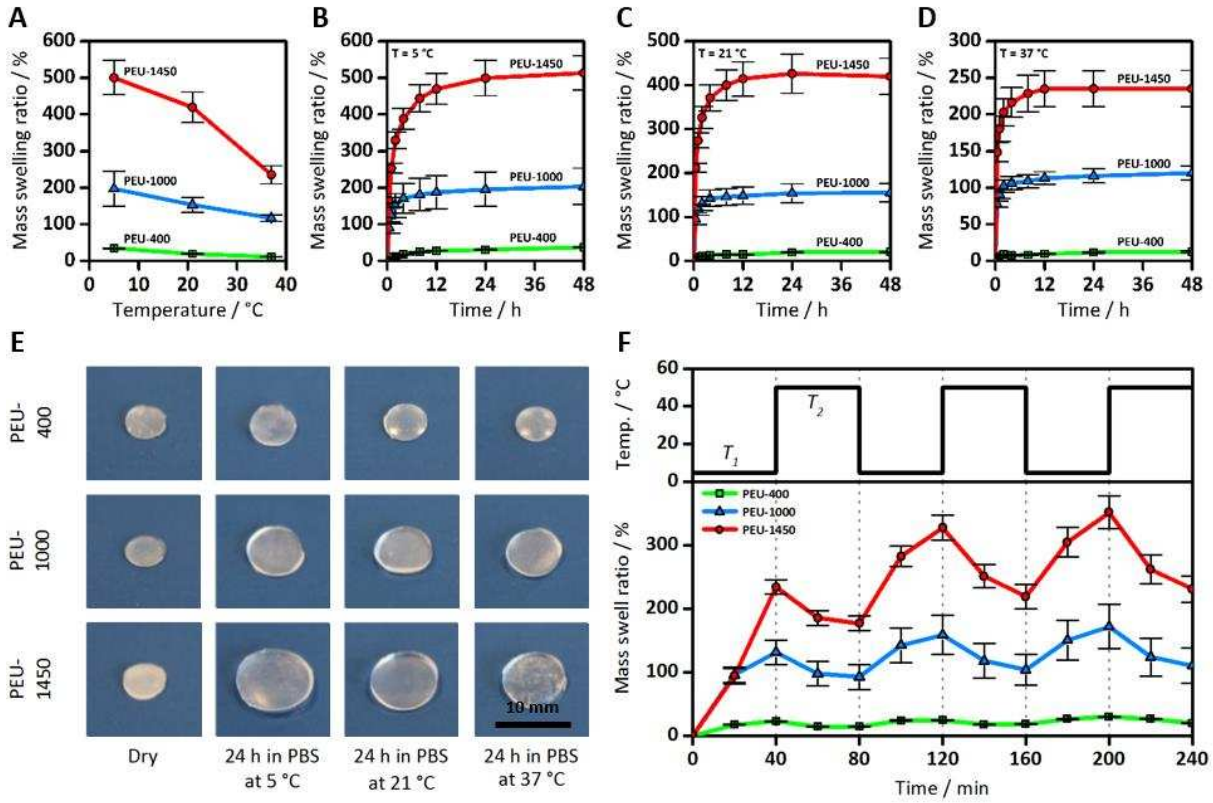

Figure 5. (A) Equilibrium ratio of swelling of PEU specimens in PBS solution as a function of the temperature. (B) Hydration kinetics of PEU samples at 5 °C, (C) 21 °C and (D) 37 °C for 2 days. (E) Pictures of PEU specimens after 24 h hydration at 5 °C, 21 °C and 37 °C. (F) Dynamic swelling/deswelling behaviour of PEU specimens at 5 °C and 50 °C at an interval of 40 min.

3.4 *In Vitro* Degradation

The biodegradability of thermoresponsive hydrogels is an important factor for potential biomedical applications.[3,7] *In vitro* degradation studies were performed in PBS with or without lipase for up to 31 days at 37 °C in a shaker bioincubator (Figure 6 and S7). The results illustrate

that the rate of degradation of the PEUs can be tuned, depending on the MWt of the PEG segments. The higher MWt PEGs showed faster degradation over the 31 days studied and this was only slightly enhanced in the presence of the enzyme (which catalyses the hydrolysis of the ester bonds of the PGS segments).[31,32] The PEUs showed bulk degradation, attributable to their high water content, in which an increase in the PEG MWt, as well as the presence of lipase led overall to a greater mass loss. PEU-400 underwent similar mass losses of 10.1% and 10.7% in 31 days in the enzyme-free and lipase-containing PBS solution, respectively. PEU-1000 and PEU-1450 underwent mass losses of 8.4% and 16.3% in 31 days in the enzyme-free PBS solution, which increased to 12.9% and 20.7%, respectively, with statistical significance, in the lipase-containing solution.

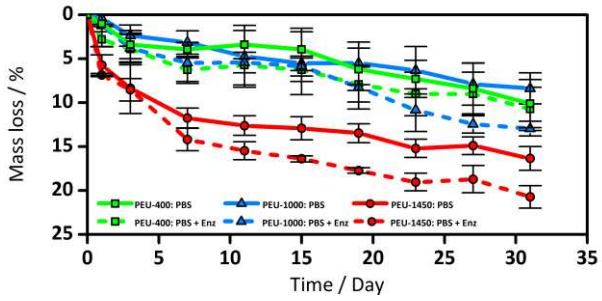

Figure 6. Percentage of mass loss of PEU specimens incubated in PBS solutions with or without lipase in a shaker incubator for up to 31 days at 37 °C.

Together with the matched mechanical properties discussed above, biodegradability enables the potential application of the PEUs in soft tissue engineering.[1,3-5] The use of PNIPAm-based hydrogels and its copolymers in biomedical applications are restricted, due to non-biodegradability and toxicity of PNIPAm in its monomeric form.[4,5,49] In comparison to recently developed PGS-co-PEG block copolymers,[24,27] the PEU hydrogels presented slower degradation kinetics owing to the urethane linkages in the covalently crosslinked network. For instance,

enzyme-free in vitro degradation tests of the PGS-co-PEG block copolymers gave ~15-80% mass losses in 21 days.[24] According to prior studies,[27,50] the use of higher MWt PEGs in in vivo applications is preferred within the test range (< 40,000 or 60,000 g mol^{-1}) which showed that high levels of low MWt PEGs (≤ 400 g mol^{-1}) led to adverse renal effects in human and animal experiments.

3.5 *In Vitro* Cell Viability and Proliferation

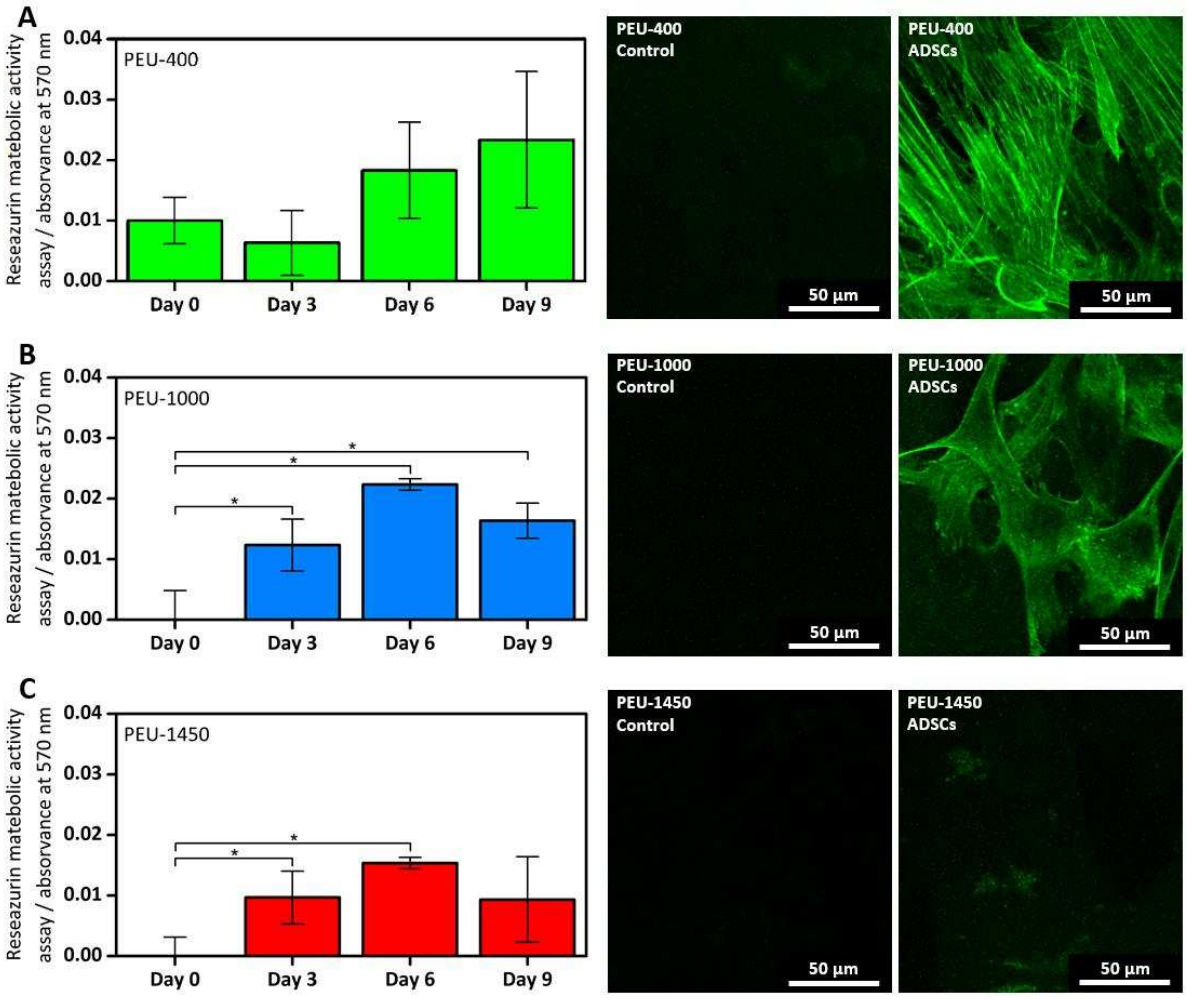

Figure 7. Metabolic activity assay results of ADSCs cultured on (A) PEU-400, (B) PEU-1000 and (C) PEU-1450 after subtracting the data for cell-free PEU controls. The data are represented

as mean ± SD (n = 3; ∗ = $p < 0.05$, two-sample t-test). The images on the right are representative confocal fluorescence micrographs following 9 days in vitro cultivation.

Metabolic activity assay with resazurin was used to evaluate the in vitro cell viability and proliferation of ADSCs (Figure 7A-C) and FIBs (Figure S8) on PEU hydrogels for up to 9 days, while confocal fluorescence microscopy was performed for cell morphology analysis (Figure 7A-C and S8). The PEU hydrogels showed no evidence of toxicity to either ADSCs or FIBs. Two-way ANOVA found significant difference between the metabolic activities of ADSCs ($p < 0.0001$) and FIBs ($p < 0.05$) in respect to the test time, while no difference in metabolic activities was found between the different PEU hydrogels. Two-sample t-test ($p < 0.05$) found PEU-1000 and PEU-1450 hydrogels presented a significant increase in metabolic activity for both cell types from day 0 to day 6 or 9, while both cell types showed statistically insignificant metabolic activities on the PEU-400 hydrogels. Maximum metabolic activity was achieved for both seeded cell types at day 6 without significant differences between day 6 and 9. ADSCs exhibited the highest metabolic activity on PEU-1000 hydrogels at day 6 (73% increase compared to day 0 cell-seeded specimens), while FIBs demonstrated the highest metabolic activity on PEU-1450 hydrogels at day 6 (51% increase compared to day 0 cell-seeded specimens). The colorimetric measurements were visually confirmed by the color change of the blue resazurin dye, with a clear change to a purple color (resorufin) for both cell types on all PEU hydrogels from day 0 to day 9 (Figure S9). The reduction of blue resazurin to purple resorufin was only seen when living cells were present (cell-free control specimens always remained blue). In contrast, the cell-seeded area on PEU-400 and PEU-1000 hydrogels turned in a distinct pink color, confirming the presence of cells on the surfaces and indicating similar metabolic activities between days 6 and 9 (Figure 7A-C and Figure S8). In contrast, the surfaces of the cell-seeded PEU-1450 hydrogels

had less visible color alterations for both cell types after cell seeding (Figure S9), as discussed below.

The confocal microscopic analysis showed elongated morphologies of the ADSCs attached to the surface of PEU-400 and PEU-1000 hydrogels and verified highly confluent cell populations (Figure 7A-B). FIBs also exhibited elongated morphologies on the PEU-400 and PEU-1000 hydrogel surfaces, however, the PEU-400 hydrogels facilitated a higher degree of confluence compared to the PEU-1000 hydrogels (Figure S8). The surfaces of the PEU-1450 hydrogels showed relatively few ADSCs and FIBs (Figure 7C and Figure S8) in line with the colorimetric measurements. This may be the result of cell detachment from the PEU hydrogels. It is likely that the temperature changes of approximately ±16 °C during the culture period (triggered by moving the samples from the incubator to the sterile laminar flow hood for medium changes and resazurin incubations) would have resulted in volume alterations of the thermosensitive PEU specimens, causing the detachment of cells from the hydrogels.[51-54] In these experiments any detached cells would then be able to proliferate on the surrounding well plate surfaces. The swelling/deswelling rates in response to temperature changes were in the order of PEU-1450 > PEU-1000 > PEU-400, and correspondingly the degree of cell detachment was highest in PEU-1450.

Overall, the above results showed that the ADSCs and FIBs proliferated on the PEU hydrogels, indicating that the PEU hydrogels had no toxic effects on the cells within this test period of 9 days. These results are consistent with previous studies on thermoresponsive and shape-changing hydrogels where a deliberate change in temperature is then used to release cell sheets for subsequent use.[51-54]

3.6 Drug Loading and Release

These thermoresponsive PEU hydrogels can also be used for drug delivery applications.[48] The release of the model drug, lidocaine, from PEU hydrogels at 37 °C was assessed using UV-Vis spectroscopy. PEUs were loaded with the drug at 5 °C, to enhance the swelling ratio and thus the amount of drug loaded into the hydrogels. The release profile of PEUs showed a rapid release within the first 4 h, followed by a reduced and sustained drug release in the proceeding time (Figure 8). PEU-400, PEU-1000 and PEU-1450 hydrogels obtained maximum drug release of 15.8% (0.37 mg ml^{-1}), 29.4% (0.70 mg ml^{-1}) and 61.2% (1.62 mg ml^{-1}) after 168 h, respectively. The initial rapid release was presumably caused by a higher drug concentration on the outer layer of the samples[55] and their shrinkage because of the higher test temperature than the drug-loading temperature. The subsequent decelerated drug release can be associated with the less permeable hydrogel matrix[48] and reduced releasable drug content over time. These results demonstrated the prospective use of the PEUs in temperature-controlled or sustained drug delivery. With a modulated volume phase transition temperature (Figure S10), the PEU hydrogels could also potentially feature an temperature dependent on-off drug release.[1,3]

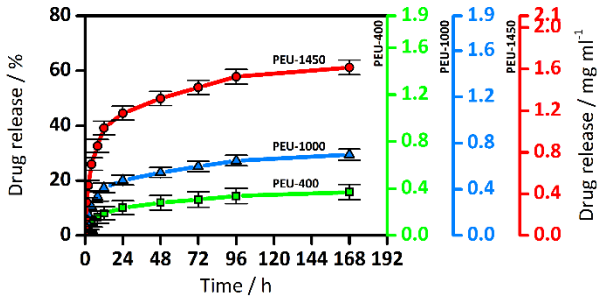

Figure 8. (A) Cumulative drug release from PEUs versus swelling time at 37 °C in PBS solution in a shaker incubator.

3.7 Water-temperature Activated Force Generation and Motions

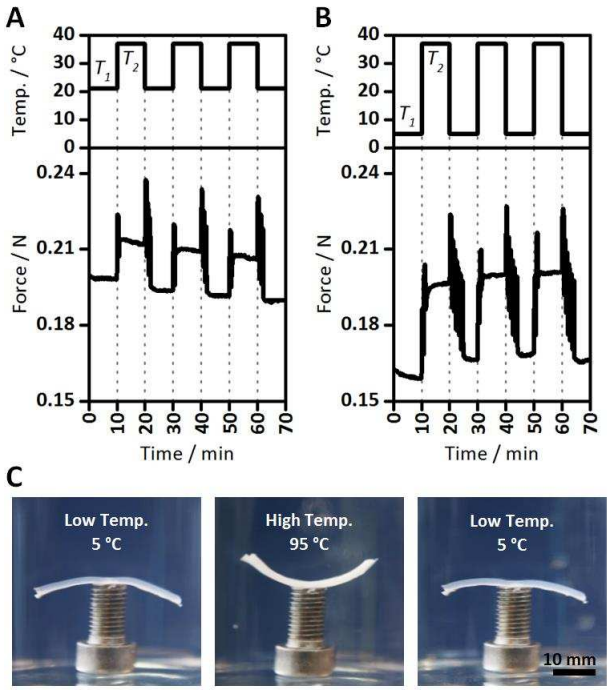

Figure 9. (A) Water temperature activated force generation of submerged and stretched PEU-1450 strip samples by cyclic alteration of water temperature from T_1 = 21 °C to T_2 = 37 °C, or from (B) T_1 = 5 °C to T_2 = 37 °C (sharp peaks = replacement of an equal volume of water with the pre-determined temperature to achieve the target temperature T_1 or T_2). (C) Water temperature responsive cantilever composed of a PEU-1450 and a PTFE film strip, transducing the water temperature dependent swelling/deswelling response into reversible bending motions.

Thermoresponsive hydrogels can also be used for actuation and power generation.[1,56] PEU-1450 hydrogels at 40% strain generated temperature-induced contractile forces and stresses (Figure 9A-B and S1). The cyclic change of water temperature from 21 °C to 37 °C and from 5 °C to 37 °C generated contractile forces of 16 ± 1 mN and 44 ± 1 mN, and stresses of 1.4 ± 0.03 kPa and 3.8 ± 0.06 kPa, respectively. Generation of the contractile forces occurred instantly upon temperature alteration and was reversible. Their values are affected by the specimen dimensions

(e.g. the specific surface area), water temperature difference, environmental conditions and swelling/deswelling capability of the PEU hydrogel. Higher contractile forces are achievable by altering these parameters, which could then be used to generate ultralow power by attaching a piezoelectric element to drive a micro- or nano-device.[56] The excellent stimuli-responsiveness of the PEU-1450 hydrogel also allowed for the design of water temperature-activated cantilevers (Figure 9C and S1), transducing the temperature-stimulus into reversible bending (see Movie S1). These characteristics will enable the PEU hydrogels to be used in actuators, sensors, soft robotics and fluid control devices.[1]

The results presented here demonstrate the successful synthesis of thermoresponsive, stretchable, biodegradable and biocompatible PEU hydrogels with tunable physiochemical properties for a variety of possible applications. The chemically crosslinked PEU hydrogels have structurally stable and highly stretchable characteristics, which may prove useful in mechanically dynamic environments for soft tissues.[4,5] Conventional thermoresponsive PNIPAm-based hydrogels are comparably less ductile, characterized with low elongation at break values of ~50%,[57-60] restraining their scope of potential applications in soft tissue engineering. Furthermore, the PEU hydrogels exhibited softer and/or more flexible properties in comparison to hydrated PGS-co-PEG block copolymers,[24] which presented a Young's modulus, tensile strength and elongation at break in the range of 0.013-1.55 MPa, 0.012-0.30 MPa and ~25-200%, respectively.[24]

The biodegradability and biocompatibility are critical aspects for developing thermosensitive PU-based hydrogels for biomedical applications. Further critical examination in vivo is needed to assess the potential for PEU hydrogels in soft tissue engineering and/or drug delivery applications, along with their prospective use in the development of bioresorbable actuators.[60] Future work can also include fabrication of the PEU hydrogels into different structures to address

the needs of different applications. In a proof-of-concept study, the fabrication of the PEU into microspheres with a size range of 289 ± 42 μm was achievable by using an oil-in-oil solvent evaporation technique (See Supplemental Information for the preparation procedure),[61] which also presented negative thermo-sensitivity (Figure 10A and Figure S11). Injectable microspheres are interesting for localized drug delivery and targeted soft tissue engineering applications.[62] The proof-of-concept production of large 3D scaffold constructs via freeze-drying (See Supplemental Information for the preparation procedure)[31,32] was also realizable, producing highly porous and interconnected microstructures (Figure 10B and Figure S11) and demonstrating great potential for further optimization of the pore size and porosity for soft tissue engineering applications.

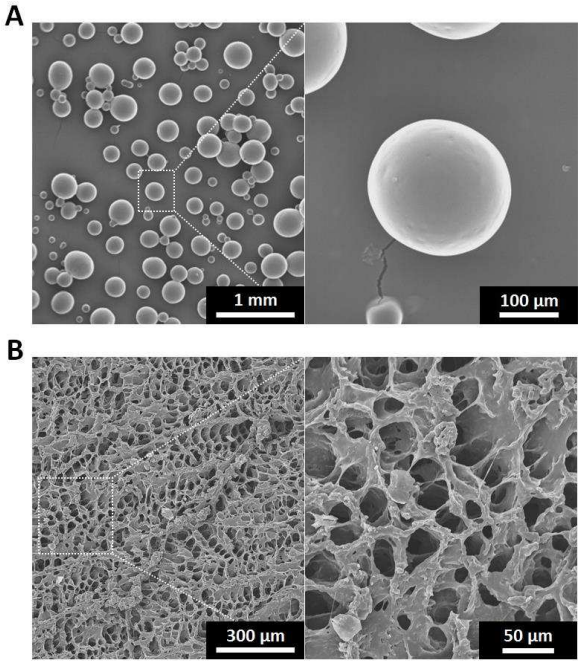

Figure 10. SEM images of (A) dry PEU-1000 microspheres, and (B) the microstructure dry PEU-1450 scaffold, both fabricated in a proof of concept study.

4. CONCLUSIONS

Thermoresponsive, stretchable, biodegradable and biocompatible PEU hydrogels with varying MWt of PEG were synthesized by a facile solvent-based two-step method. The chemical and physical characteristics of the covalently crosslinked PEU hydrogels are tunable by changing the MWt of the PEG segments. PEU hydrogels were processed into films, with structurally stable and highly stretchable mechanical properties in dry and hydrated states. The PEU hydrogels were characterized with a tensile Young's modulus, ultimate tensile strength and elongation at break in the range of 0.02-0.20 MPa, 0.05-0.47 MPa and 426-623%, respectively. Compression tests showed no fracture and good recoverability after 75% axial strain. The PEU hydrogels demonstrated minimal hysteresis loss ratio during cyclic tensile tests, while cyclic compression tests showed higher hysteresis loss ratios. The PEU hydrogels were characterized with negative thermo-sensitivity, and the equilibrium ratio of swelling depended on the medium temperature and PEU composition. The PEU hydrogels demonstrate repetitive and reversible responses to changes in medium temperature from 5 ^{o}C to 37 ^{o}C with the swelling ratio at equilibrium varying from 499% to 12%. In vitro degradation tests of PEU hydrogels obtained mass losses of 9-16% or 11-21% in 31 days in PBS or lipase solution, respectively. *In vitro* cell test results provided clear evidence that all the PEU hydrogels are biocompatible and suitable for the culture of ADSCs and FIBs.

The PEU hydrogels showed a rapid drug release within the first hour in PBS, followed by a sustained drug release rate in the proceeding time and reaching a maximum drug release in the range of 16-61% after 168 h. Water temperature activated force generation of submerged and stretched PEU strip samples generated contractile forces of 16 ± 1 mN and 44 ± 1 mN and stresses of 1.4 ± 0.03 kPa and 3.8 ± 0.06 kPa by cyclic water temperature changes, which

occurred instantly upon temperature alteration and was reversible. The proof-of-concept fabrication of structures such as PEU microspheres and large 3D scaffolds illustrates versatility of the polymers. The thermoresponsivity, high flexibility and stretchability, biodegradability and biocompatibility show the potential of the PEU hydrogels to be applied in a variety of applications such as soft tissue engineering, temperature-controlled or sustained drug delivery as well as thermal actuation.

ASSOCIATED CONTENT

Supporting Information

The Supporting Information includes: Determination of the Effective Crosslink Density; Proof-of-concept preparation procedure of PEU microspheres; Proof-of-concept preparation procedure of PEU scaffolds; Schematic illustrations of test setups (Figure S1); ^{1}H NMR spectra of PEGs and pre-PGS (Figure S2); ATR-FTIR spectra of pre-PGS, PEGs and NCO-terminated PEG pre-polymer (Figure S3); Raman spectra of pre-PGS and PEGs (Figure S4); DSC curves of pre-PGS and PEGs (Figure S5); Images of the compression behavior of PEUs (Figure S6); SEM micrographs of PEUs: untreated and after *in vitro* degradation (Figure S7); Metabolic activity assay confocal and fluorescence micrographs of FIBS (Figure S8); In vitro cell test images (Figure S9); Evaluation of the volume phase transition temperature of PEUs (Figure S10); Images of the swelling/deswelling behavior of PEU-1000 microspheres. Image of dry PEU-1450 scaffold specimen (Figure S11). This material is available free of charge via the Internet at http://pubs.acs.org.

AUTHOR INFORMATION

Corresponding Author

*E-mail: biqiong.chen@sheffield.ac.uk. Fax: +441142225943. Tel: +441142225958.

Notes

The authors declare no competing financial interest.

ACKNOWLEDGMENTS

We thank the University of Sheffield for a start-up package and the Royal Society for financial support (RG120037).

REFERENCES

(1) K. Deligkaris, T.S. Tadele, W. Olthuis and A. van den Berg, *Sensor. Actuat. B-Chem.* **2010**, *147*, 765.

(2) J. Zhu and R.E. Marchant, *Expert. Rev. Med. Devices*. **2011**; *8*, 607.

(3) L. Klouda and Mikos, A.G. *Eur. J. Pharm. Biopharm.* **2008**, *68*, 34.

(4) H.L. Lim, Y. Hwang, M. Kar and S. Varghese, *Biomater. Sci.* **2014**, *2*, 603.

(5) A.B. Imran, T. Seki and Y. Takeoka, *Polym. J.* **2010**, *42*, 839.

(6) H. Fu, H. Gao, G. Wu, Y. Wang, Y. Fan and J. Ma, *Soft Matter* **2011**, *7*, 3546.

(7) R. París, Á. Marcos-Fernández and I. Quijada-Garrido, *Polym. Adv. Technol.* **2013**, *24*, 1062.

(8) S.A. Guelcher, *Tissue Eng. Part B* **2008**, *14*, 3.

(9) A.K. Bajpai, S.K. Shukla, S. Bhanu and S. Kankane, *Prog. Polym. Sci.* **2008**, *33*, 1088.

(10) M. Mehdizadeh and J. Yang, *Macromol Biosci.* **2013**, *13*, 271.

(11) X. Sun, H. Gao, G. Wu, Y. Wang, Y. Fan and J. Ma, Int. J. Pharm. **2011**, 412, 52.

(12) J. Zhu, *Biomaterials* **2010**, *31*, 4639.

(13) B.V. Slaughter, S.S. Khurshid, O. Fisher, A. Khademhosseini and A.N. Peppas, Adv. Mater. **2009**, 21, 3307.

(14) S.H. Chen, C.T. Tsao, C.H. Chang, Y.M. Wu, Z.W. Liu, C.P. Lin, C.K. Wang and K.H. Hsieh, Carbohydr. Polym. **2012**, 88, 1483.

(15) R. Li, N. Liu, B. Li, Y. Wang, G. Wu and J. Ma, Polym. Chem. **2015**, 6, 3671.

(16) X.J. Loh, K.B.C. Sng and J. Li, Biomaterials **2008**, 29, 3185.

(17) Y. Wang, G.A. Ameer, B.J. Sheppard and R. Langer, *Nat. Biotechnol.* **2002**, *20*, 602.

(18) R. Rai, M. Tallawi, A. Grigore and A.R. Boccaccini, *Prog. Polym. Sci.* **2012**, *37*, 1051.

(19) Q.Z. Chen, A. Bismarck, U. Hansen, S. Junaid, M.Q. Tran, S.E. Harding, N.N. Ali and A.R. Boccaccini, *Biomaterials* **2008**, *29*, 47.

(20) I.H. Jaafar, M.M. Ammar, S.S. Jedlicka, R.A. Pearson and J.P. Coulter, J. Mater. Sci. **2010**, 45, 2525.

(21) Y. Wang, Y.M. Kim and R. Langer, *J. Biomed. Mater. Res. A.* **2003**, *66*, 192.

(22) I. Pomerantseva, N. Krebs, A. Hart, C.M. Neville, A.Y. Huang and C.A. Sundback, *J. Biomed. Mater. Res. A*, **2009**, 91, 1038.

(23) M.J.N. Pereira, B. Ouyang, C.A. Sundback, N. Lang, I. Friehs, S. Mureli, I. Pomerantseva, J. McFadden, M.C. Mochel, O. Mwizerwa, P. del Nido, D. Sarkar, P.T. Masiakos, R. Langer, L.S. Ferreira and J.M. Karp, *Adv. Mater.* **2013**, *25*, 1209.

(24) A. Patel, A.K. Gaharwar, G. Iviglia, H. Zhang, S. Mukundan, S.M. Mihaila, D. Demarchie and A. Khademhosseini, *Biomaterials* **2013**, *34*, 3970.

(25) T. Wu, M. Frydrych, K. O'Kelly and B. Chen, *Biomacromolecules* **2014**, *15*, 2663.

(26) Q.Y. Liu, S.Z. Wu, T.W. Tan, J.Y. Weng, L.Q. Zhang, L. Liu, W. Tian and D.F. Chen, *J. Biomater. Sci. Polym. Ed.* **2009**, *20*, 1567.

(27) Y. Wu, L. Wang, B. Guo and P.X. Ma, *J. Mater. Chem. B.* **2014**, *2*, 3674.

(28) W. Cai and L. Liu, *Mater. Lett.* **2008**, 62, 2171.

(29) J. Tuominen, J. Kylmä, A. Kapanen, O. Venelampi, M. Itävaara and J. Seppälä, *Biomacromolecules* **2002**, *3*, 445.

(30) J. Gao, P. Crapo and Y. Wang, *Tissue Eng.* **2006**, *12*, 917.

(31) M. Frydrych and B. Chen, *J. Mater. Chem. B* **2013**, *1*, 6650.

(32) M. Frydrych, S. Román, S. MacNeil and B. Chen, *Acta Biomater.* **2015**, *18*, 40.

(33) J.S. Chawla and M.M. Amiji, *Int. J. Pharm.* **2002**, *249*, 127.

(34) D.R. Ralston, C. Laytont, A.J. Dalley, S.G. Boyce, E. Freedlander and S. MacNeil, Br. J. Plast. Surg. **1997**, 50, 408.

(35) C.L.E. Nijst, J.P. Bruggeman, J.M. Karp, L. Ferreira, A. Zumbuehl, C.J. Bettinger and R. Langer, Biomacromolecules **2007**, 8, 3067.

(36) M.W. Urban, C.L. Allison, C.C. Finch and B.A. Tatro, *J. Coating Technol.* **1999**, *71*, 75.

(37) R. Maliger, P.J. Halley and J.J. Cooper-White, *J. Appl. Polym. Sci.* **2013**, *127*, 3980.

(38) D. Yamini, G. Devanand Venkatasubbu, J. Kumar and V. Ramakrishnan, *Spectrochim. Acta A* **2014**, *117*, 299.

(39) Y. Jin, M. Sun, D. Mu, X. Ren, Q. Wang and L. Wen, *Electrochim. Acta* **2012**, *78*, 459.

(40) S.Y. Moon, Y.D. Park, C.J. Kim, C.H. Won and Y.S. Lee, Bull. Korean Chem. Soc. **2003**, 24, 1361.

(41) Z. You, H. Cao, J. Gao, P.H. Shin, B.W. Day and Y. Wang, Biomaterials **2010**, 31, 3129.

(42) Y. Li, Q. Ma, C. Huang and G. Liu, Mater. Sci. **2013**, 19, 147.

(43) K. Park, W.S.W. Shalby and H. Park, *Biodegradable Hydrogels for Drug Delivery*, Technomic Publishing, Lancaster, **1993**.

(44) Ruiz, J.; Mantecón, A.; Cádiz, V. *Polymer* **2001**, *42*, 6347.

(45) A.J. Kinloch and R.J. Young, *Fracture Behaviour of Polymers*, Applied Science Publisher, London, **1983**.

(46) Q.Z. Chen, S.E. Harding, N.N. Ali, A.R. Lyon and A.R. Boccaccini, *Mat. Sci. Eng. R* **2008**, *59*, 1.

(47) A. Gefen and E. Haberman, *J. Biomech. Eng.* **2007**, *129*, 924.

(48) Y. Qiu and K. Park, *Adv. Drug Deliver. Rev.* **2012**, *64*, 49.

(49) H.G. Schild, *Prog. Polym. Sci.* **1992**, 17, 163.

(50) K. Knop, R. Hoogenboom, D. Fische, U.S. Schubert, *Angew. Chem. Int.* **2010**, 49, 6288.

(51) S.J. Kim, I. Jun, D.W. Kim, Y.B. Lee, Y.J. Lee, J.H. Lee, K.D. Park, H. Park and H. Shin, *Biomacromolecules* **2013**, 14, 4309.

(52) I. Jun, Y.B. Lee, Y.S. Choi, A.J. Engler, H. Park and H. Shin, *Biomaterials* 2015, 54, 44.

(53) O.O. Akintewe, S.J. DuPont, K.K. Elineni, M.C. Cross, R.G. Toomey and N.D. Gallant, *Acta Biomater.* **2015**, 11, 96.

(54) A. Kikuchi and T. Okano, J. Control. Release **2005**, 101, 69.

(55) X. Huang and C.S. Brazel, *J. Control. Release* **2001**, *73*, 121.

(56) M. Ma, L. Guo, D.G. Anderson and R. Langer, *Science* **2012**, *339*, 186.

(57) Y. Tan, K. Xu, P. Wang, W. Li, S. Sun and L. Dong, Soft Matter **2010**, 6, 1467.

(58) Z. Li, J. Shen, H. Ma, X. Lu, M. Shi and M. Ye, Mater. Sci. Eng. C **2013**, 33, 1951.

(59) K. Haraguchi, T. Takehisa and S. Fan, Macromolecules **2002**, 35, 10162.

(60) L. Ionov, Mater. Today **2014**, 17, 494.

(61) M. Li, O. Rouaud and D. Poncelet, *Int. J. Pharm.* **2008**, *363*, 26.

(62) N.K. Varde and D.W. Pack, *Expert Opin. Biol. Ther.* **2004**, *4*, 35.